



香港科技大学

**Hong Kong University of Science and Technology
(HKUST)**

Magnetic and transport properties in the field-induced phase transitions in Ni₅₀Mn_{50-x}In_x Heusler alloys

Zhang Xixiang

Physics,

Hong Kong University of Science and Technology

Introduction

The search for ferromagnetic materials suitable for application in semiconductor spintronics devices.

To allow efficient spin injection into the semiconductor, these materials must satisfy at least the following

- 1) Curie temperature significantly higher than the room temperature, the working temperature of semiconductors used industrially.
- 2) A very high spin polarization of the electron states at the Fermi level.

Heusler alloys were predicted to be Half-metals

VOLUME 50, NUMBER 25

PHYSICAL REVIEW LETTERS

20 JUNE 1983

New Class of Materials: Half-Metallic Ferromagnets

R. A. de Groot and F. M. Mueller

Research Institute for Materials, Faculty of Science, Toernooiweld, 6525 ED Nijmegen, The Netherlands

and

P. G. van Engen and K. H. J. Buschow

Philips Research Laboratories, 5600 JA Eindhoven, The Netherlands

(Received 21 March 1983)

The band structure of Mn-based Heusler alloys of the $C1_b$ crystal structure (MgAgAs type) has been calculated with the augmented-spherical-wave method. Some of these magnetic compounds show unusual electronic properties. The majority-spin electrons are metallic, whereas the minority-spin electrons are semiconducting.

PACS numbers: 71.10.+x, 71.25.Pi, 75.20.En

Magnetic materials based on the $L2_1$ and $C1_b$ crystallographic phases have been of interest to both theorists and experimentalists since they were first considered by Heusler.¹ His interest focused on the unusual result that some of these materials in these crystallographic phases were

structure types can be described by means of four interpenetrating fcc lattices. For the ordinary $L2_1$ Heusler alloys these fcc lattices can be characterized by the positions X_1 ($\frac{1}{4}\frac{1}{4}\frac{1}{4}$), X_2 ($\frac{3}{4}\frac{3}{4}\frac{3}{4}$), Y (000), and Z ($\frac{1}{2}\frac{1}{2}\frac{1}{2}$). The same holds for the $C1_b$ structure with the exception that the X_1 positions

Half metal

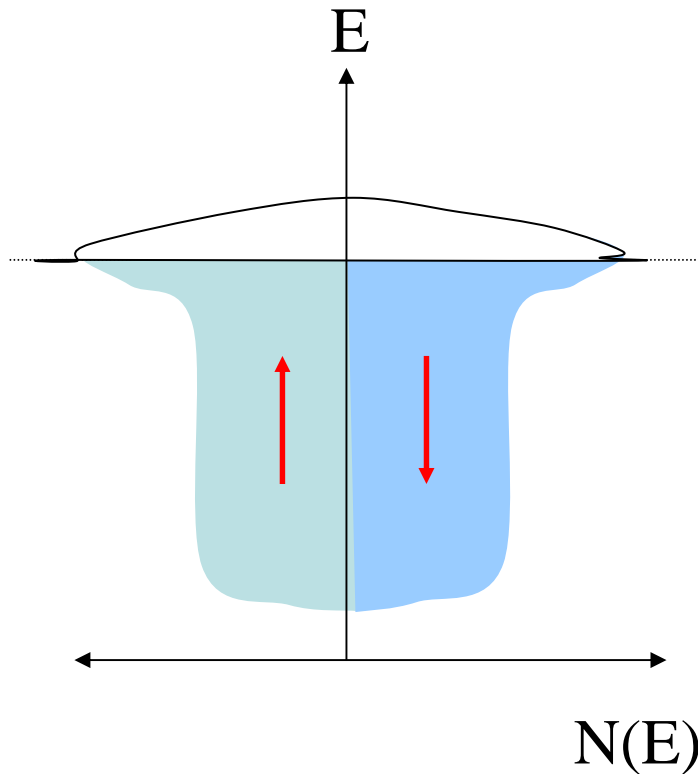
key material candidate for spintronics

$$\textit{polarization} = \frac{n_{\uparrow} - n_{\downarrow}}{n_{\uparrow} + n_{\downarrow}} = 100\%$$

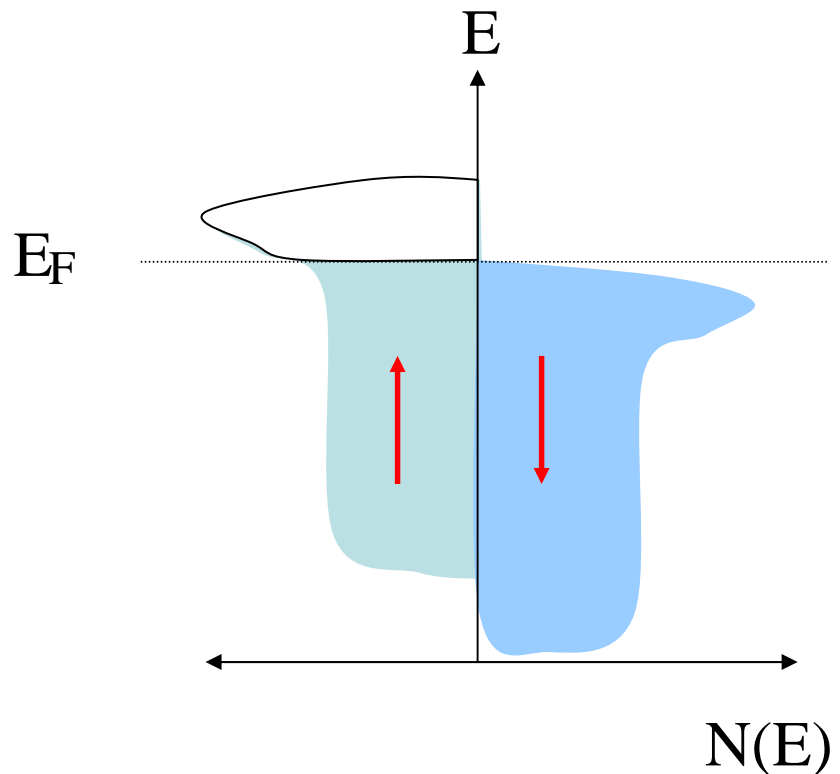
n_{\uparrow} and n_{\downarrow} are electron density

$$n_{\uparrow} \text{ Or } n_{\downarrow} = 0$$

Nonmagnetic vs. Magnetic Materials

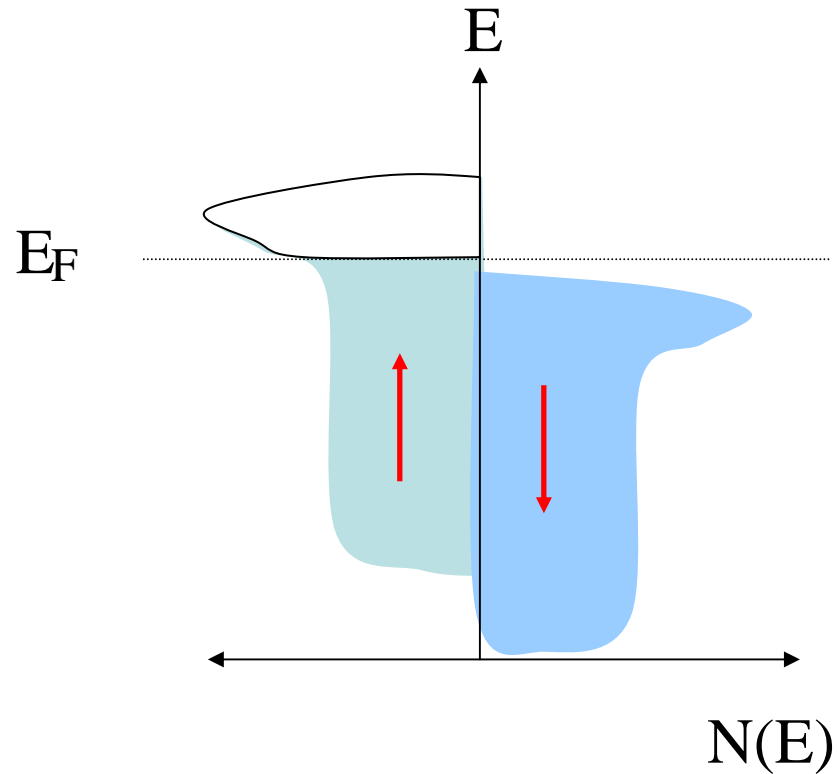


Nonmagnetic



Magnetic

Half metals



Spins of all the conducting electrons point to the same direction “Up”

Heusler alloys of Higher-spin-polarization

(much higher than the conventional ferromagnetic metals)

- spin polarization of the **Co₂MnSi** Heusler compound has been estimated to be **61%** at 10 K.
(Kammerer et al. APL85, 79,(2004))
- Point-contact Andreev reflection measurements of the spin polarization yield polarization values for **Co₂MnSi** and **NiMnSb** of **56%** and **45%**, respectively
(L. Ritchie et al., Phys. Rev. 68, 104430(2003)).

Polarization of Ferromagnetic materials

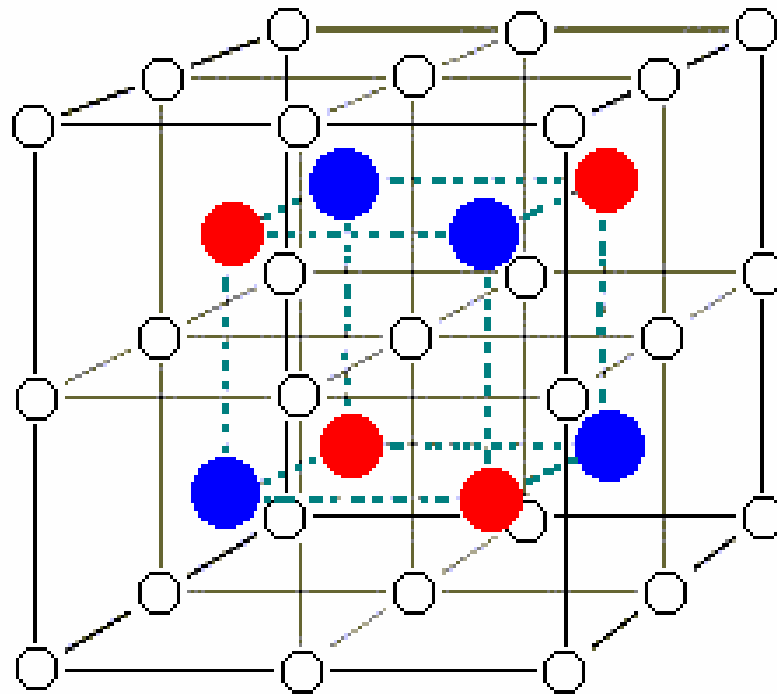
Material studied	Point	Base	N	P_T (%)	P_C (%)
NiFe	Nb	Ni _{0.8} Fe _{0.2} film	14	25 ± 2	37 ± 5
Co	Nb	Co foil	7	35 ± 3	42 ± 2
Fe	Ta	Fe film	12	40 ± 2	45 ± 2
	Fe	Ta foil	14		46 ± 2
	Nb	Fe film	4		42 ± 2
	Fe	V crystal	10		45 ± 2
Ni	Nb	Ni foil	4	23 ± 3	46.5 ± 1
	Nb	Ni film	5		43 ± 2
	Ta	Ni film	8		44 ± 4
NiMnSb	Nb	NiMnSb film	9	–	58 ± 2.3
LSMO	Nb	La _{0.7} Sr _{0.3} MnO ₃ film	14	–	78 ± 4.0
CrO ₂	Nb	CrO ₂ film	9	–	90 ± 3.6

Ferromagnetic shape memory alloys

Ferromagnetic Heusler alloys are well known ferromagnetic shape memory alloys

- Martensitic transformation
- Magnetic field induced strain
- Applications in actuators
-

Typical Heusler alloys - Ni₂MnGa



Ni



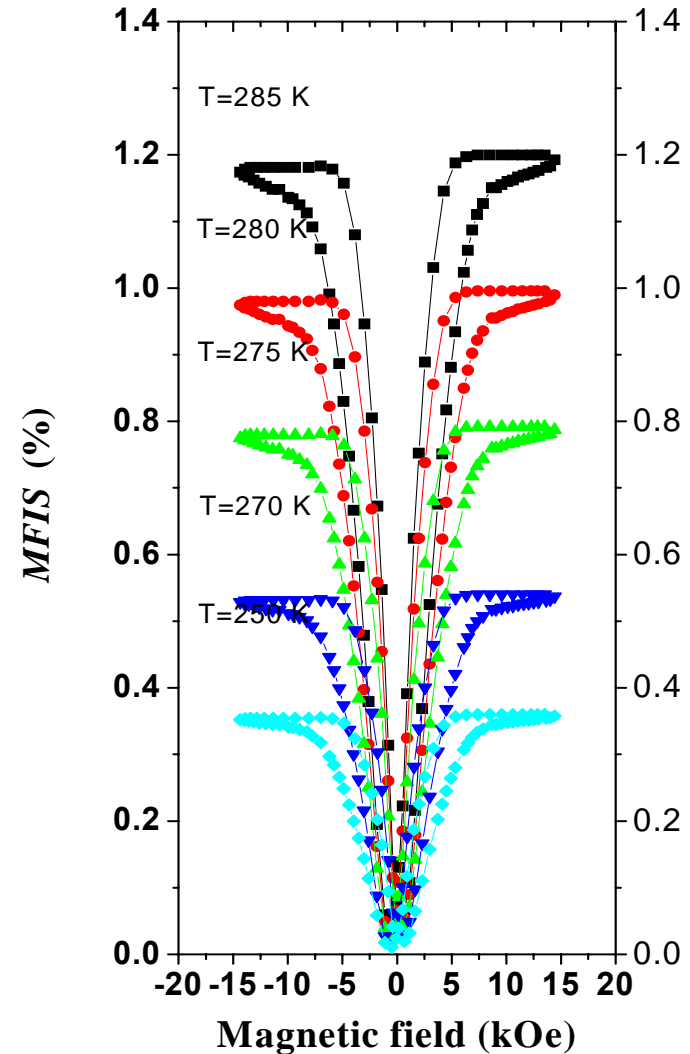
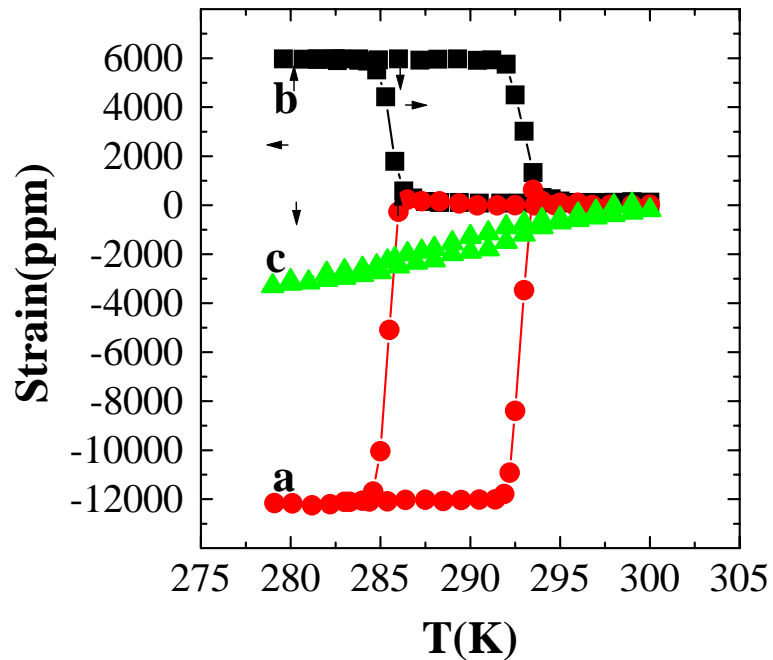
Mn



Ga

Characteristics

Thermal-elastic martensitic transformation Shape memory effect

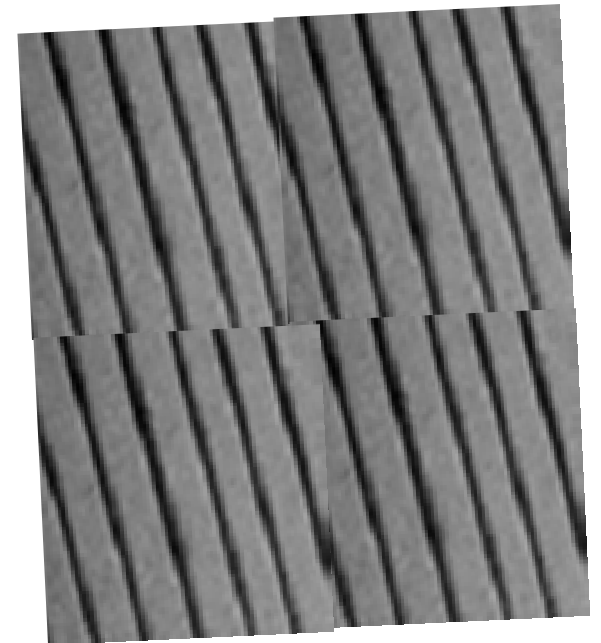


**Spontaneous shape
memory effect in single
crystals**

Mechanism of field induced strain



$H=0$



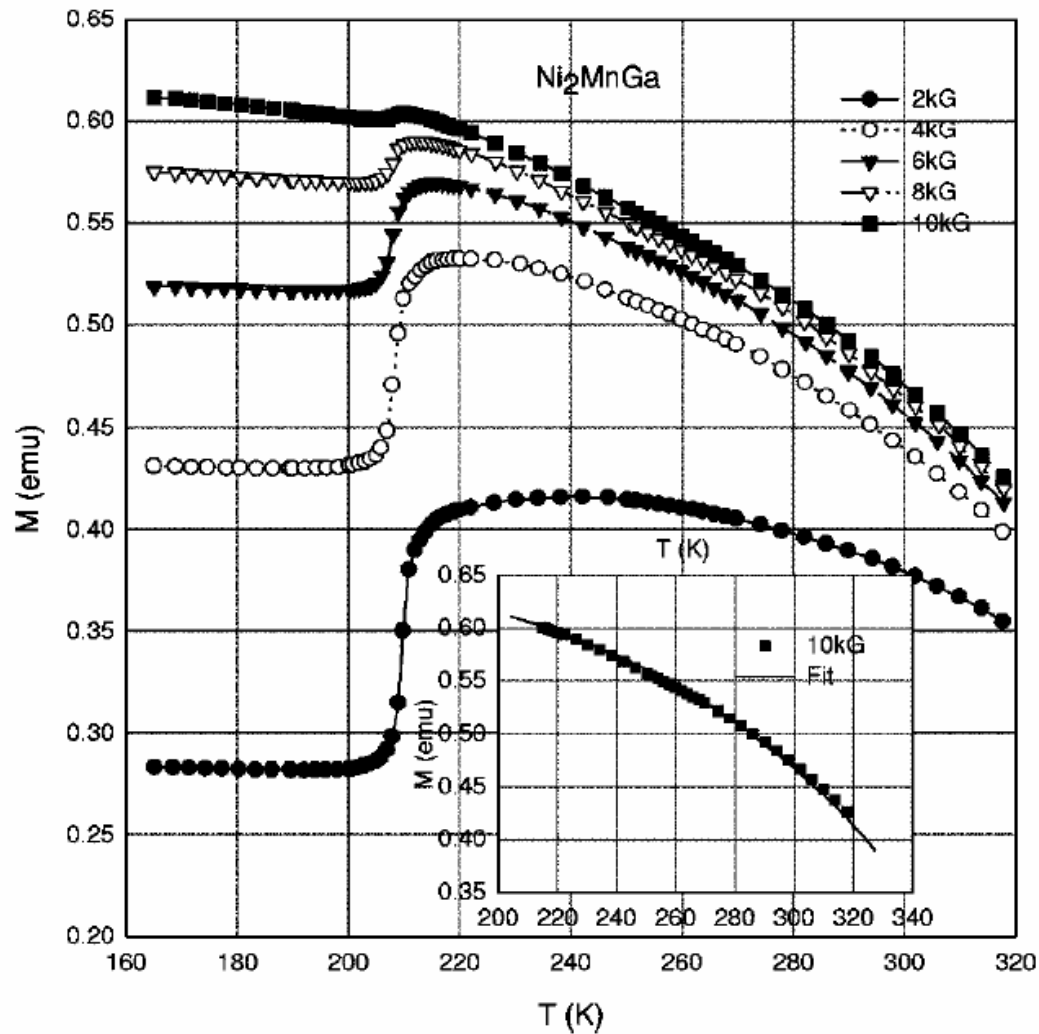
$H \geq H_A$

Characteristics of Ni₂MnGa

- **High temperature phase (or austenite)** :
ferromagnetic, low magnetic anisotropy
cubic lattice
- **Low temperature phase (martensite)**:
ferromagnetic, strong magnetic anisotropy,
tetragonal lattice
- **Both phase are ferromagnetic metals**

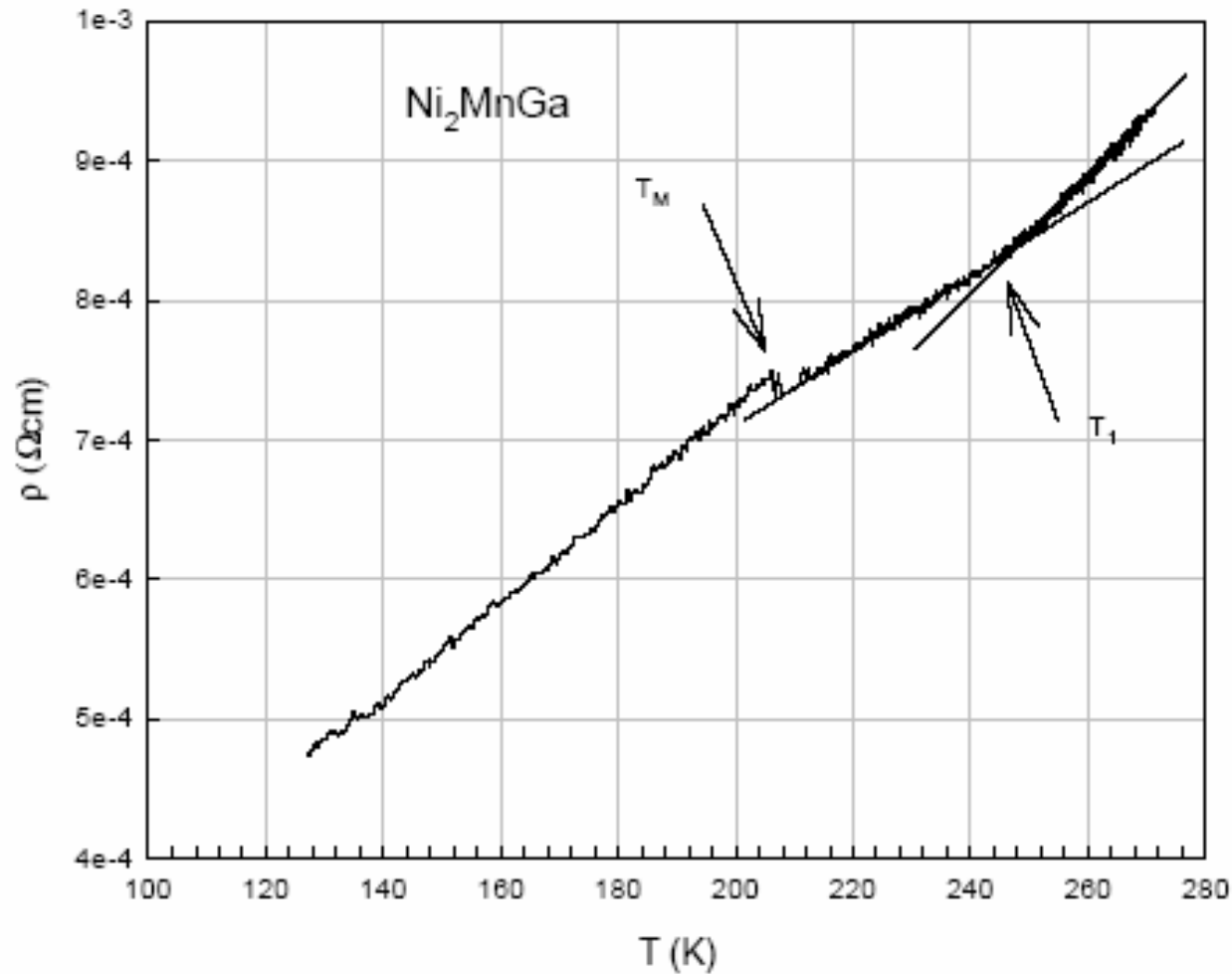
M(T) curves with different applied magnetic fields

F. Zuo et al PRB58,11127(1998)

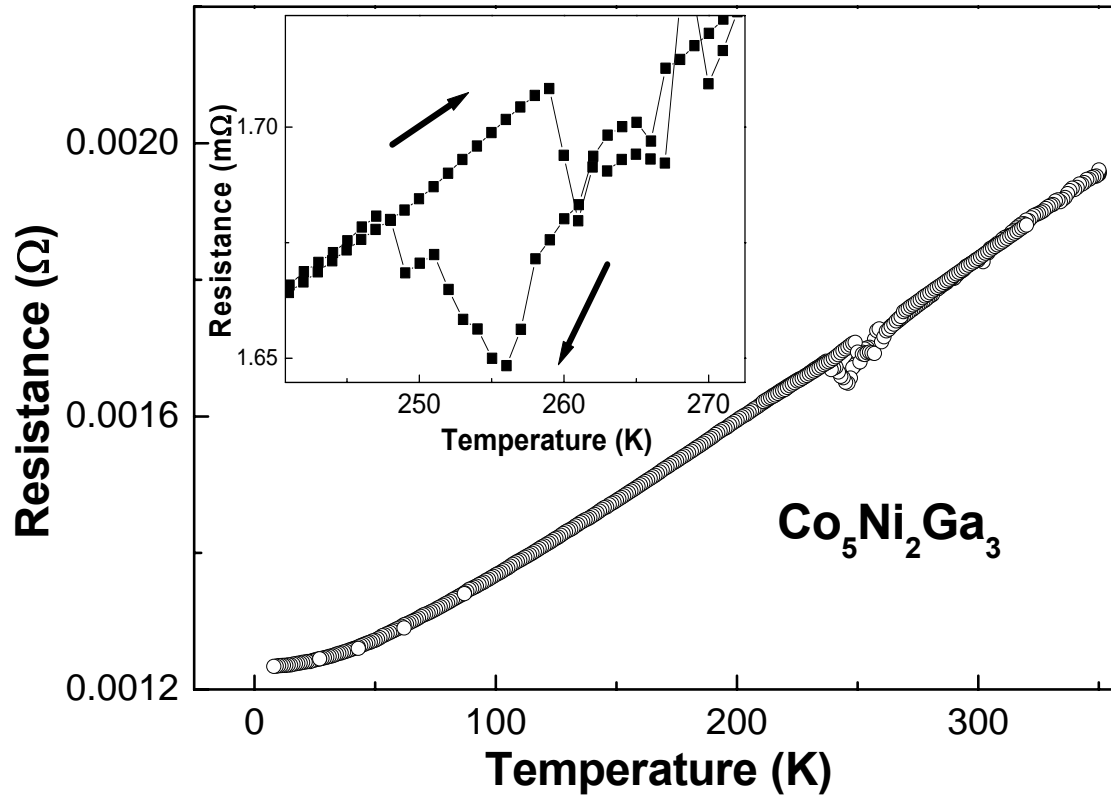


Temperature-dependent resistivity

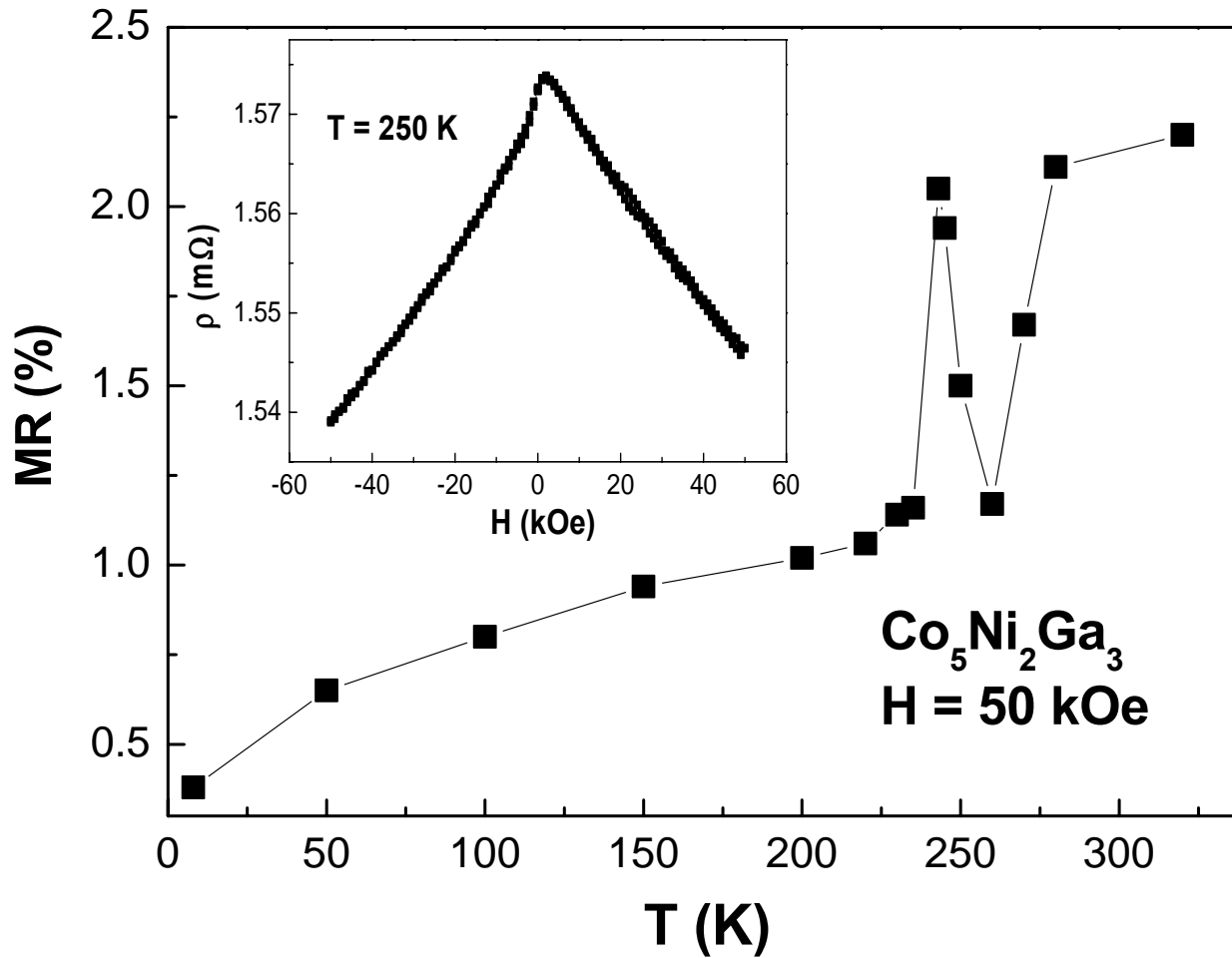
Zuo et al, J. Phys.: Condens. Matter **11** (1999) 2821–2830.)



CoNiGa alloys

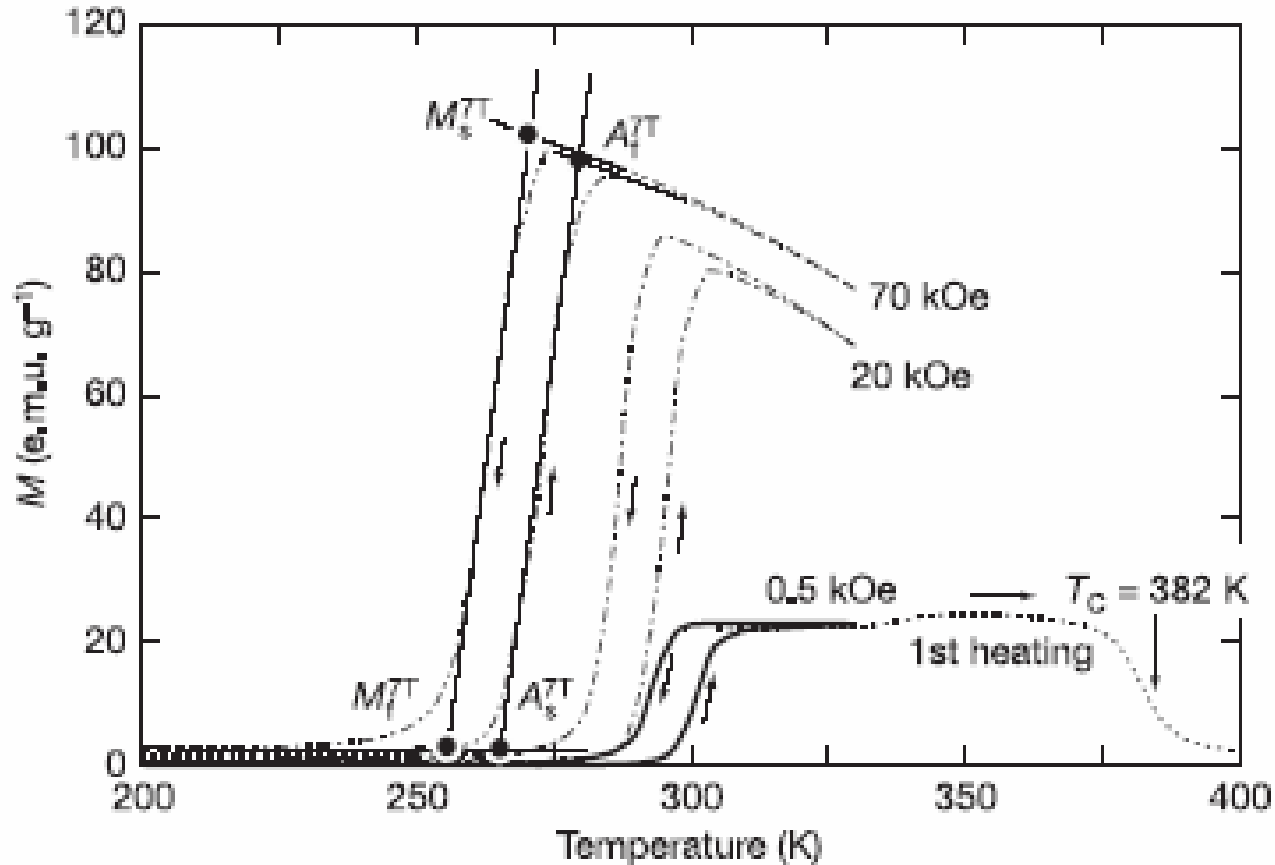


Magnetoresistance



Ni₂MnCoIn crystals

Nature 439, 957(2006)



$$E = -\vec{B} \cdot \vec{M}$$

Ni₅₀Mn_{50-x}In_x single crystals

(x=14-16.3)

- single crystals were grown at a rate of 5–30 mm/h using a Czochralski instrument with a cold crucible system
- X-ray: High temperature phase is L21-type ordered structure with a lattice constant $a=6.006\text{\AA}$.
- Cooling to 93K, the crystal structure changes to an orthorhombic structure with a rather complex martensitic modulated sub-structure.

Magnetic, electrical and thermal transport measurements

- Magnetic measurements: Quantum Design SQUID magnetometer, 2-400 K, 5 Tesla
- Transport measurements: Quantum Design Physical Property Measurement system (PPMS), 2-400 K, 9Tesls
- Specific Heat: PPMS

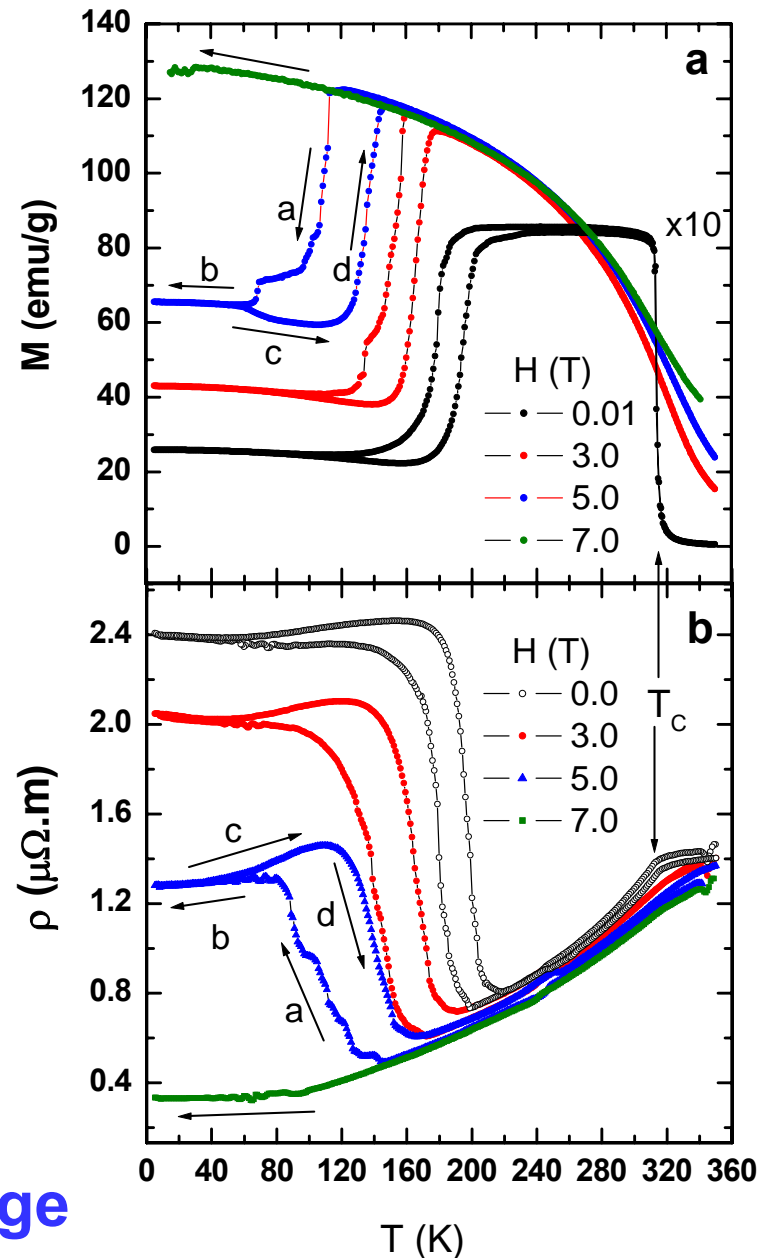
M(T) and $\rho(T)$ in different fields

(APL91,2007)

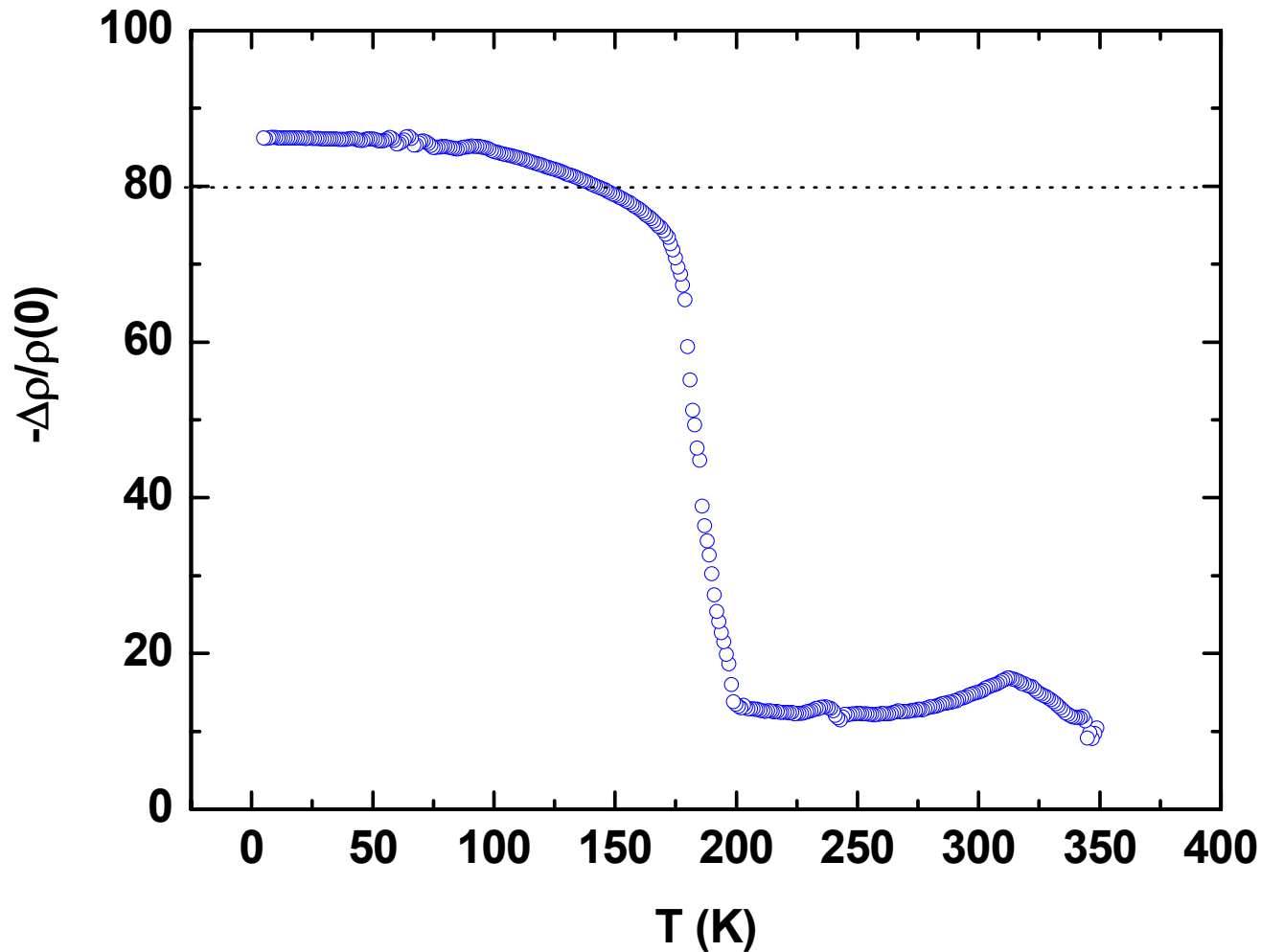
Features:

- (1) The martensitic transformation with thermal hysteresis.
- (2) Martensitic transformation is magnetic field dependent.
- (3) Magnetic field shift transition to lower temperature.
- (4) The transformation can be totally suppressed by magnetic field.
- (5) Currie temperature $T_c=315\text{K}$
- (6) Low-T martensite is ferrimagnetic, poor metal.
- (7) High T, ferromagnetic austenite, metal
- (8) Martensitic transformation is accompanied by a metal-poor metal transition.

GMR in a broad temperature range



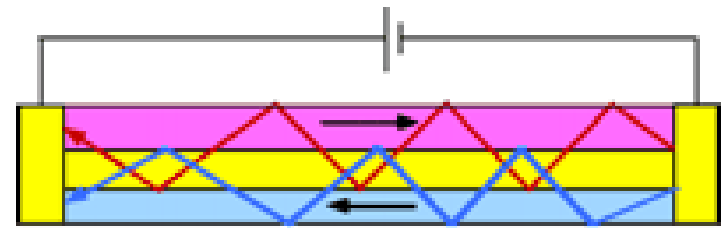
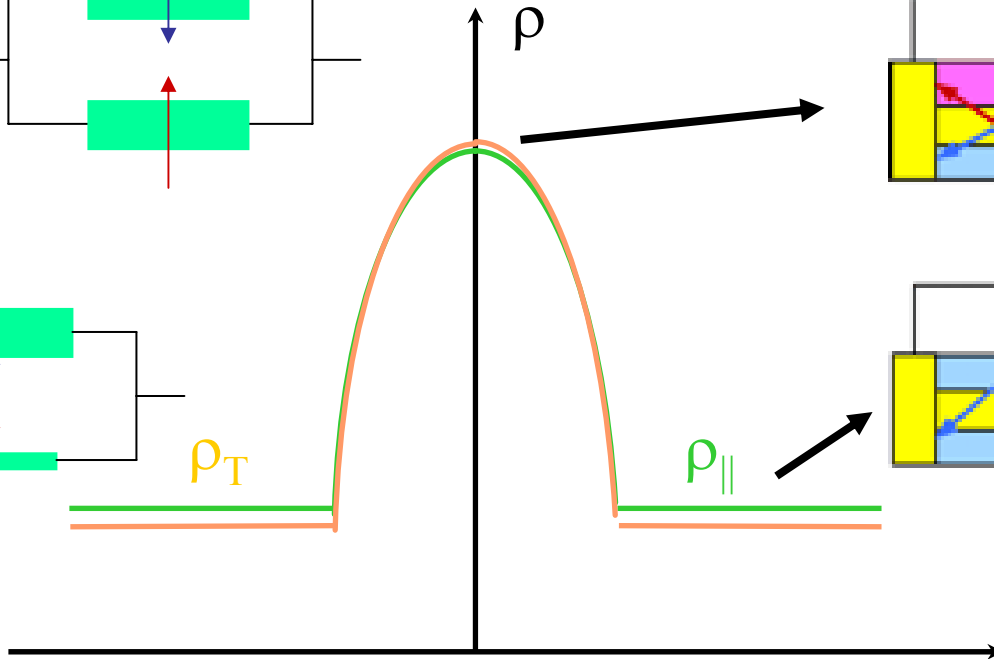
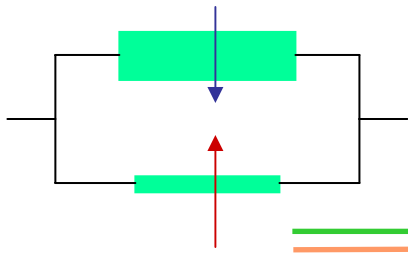
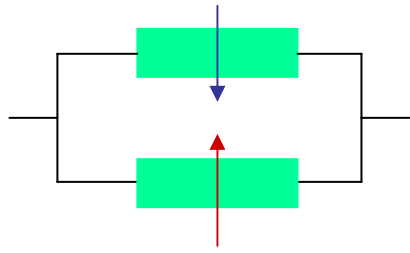
GMR in a broad temperature range



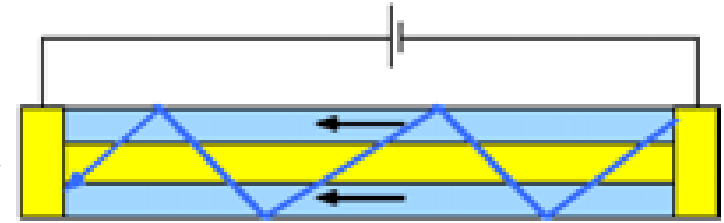
At 5K, for Crystal 1 MR =86%

Giant MR and Tunneling MR

Giant MR (GMR) $\rho_T = \rho_{||}$



High resistance



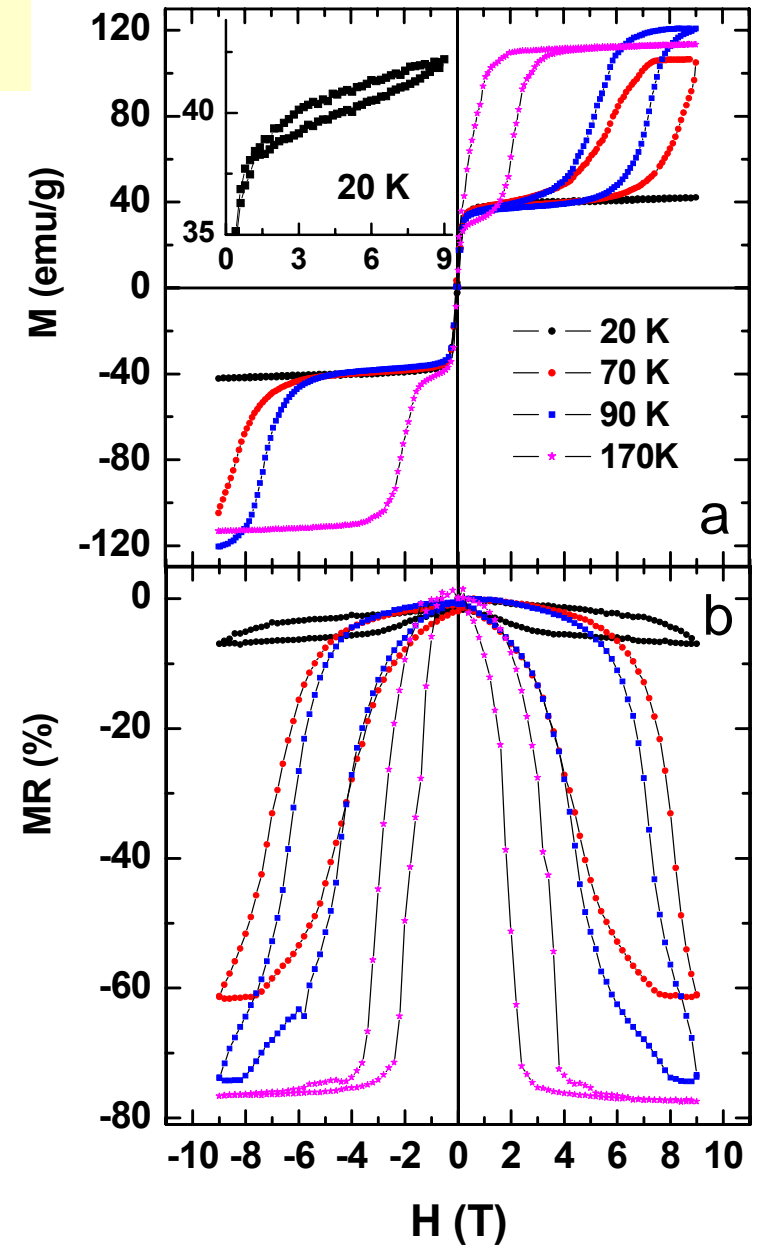
Low resistance

H

M(H) and MR(H) in different fields

M(H) curves indicate a **metamagnetic** behavior or **field-induced phase transition**

$\rho(H)$ or MR (H) has the similar transition fields



Superzone Gap

Superzone gap:

The antiferromagnetic lattice does not commensurate with the crystal lattice, which leads to a new Brillouin boundary (a gap appearing on the Fermi surface).

- In intermetallic alloys, the large MR results from the collapsing of the “superzone gap” due to field induced first order phase transition.
(UNiGa, PRL77,5253).

$\text{Ni}_{50}\text{Mn}_{33.7}\text{In}_{16.3}$ single crystal

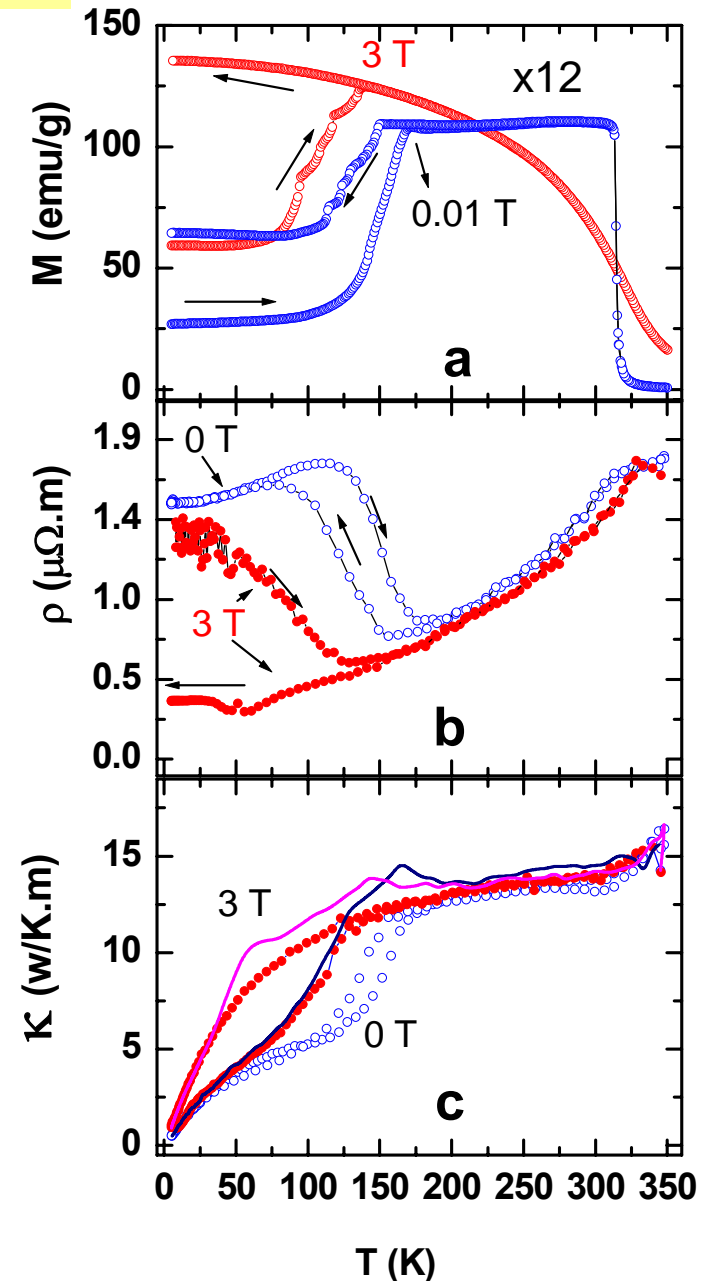
Showing the similar martensitic transformation, metal-poor metal transition, **GMR** and **Giant Thermal conductivity**.

Free electron Wiedemann-Franz law

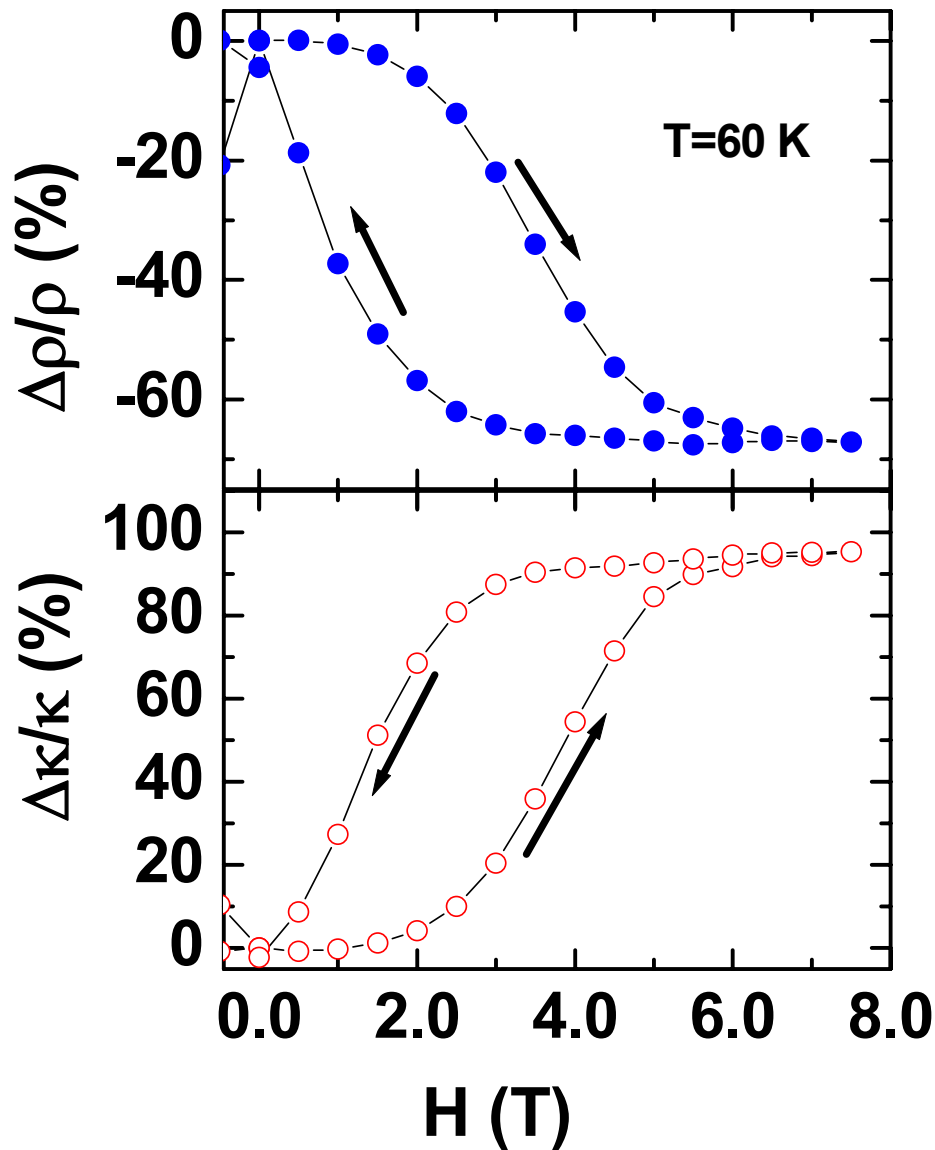
$$\frac{k}{\sigma T} = L = 2.45 \times 10^{-8} \text{ W}\Omega\text{K}^{-2}$$

the upper bound for $\Delta\kappa_{\text{el}}$

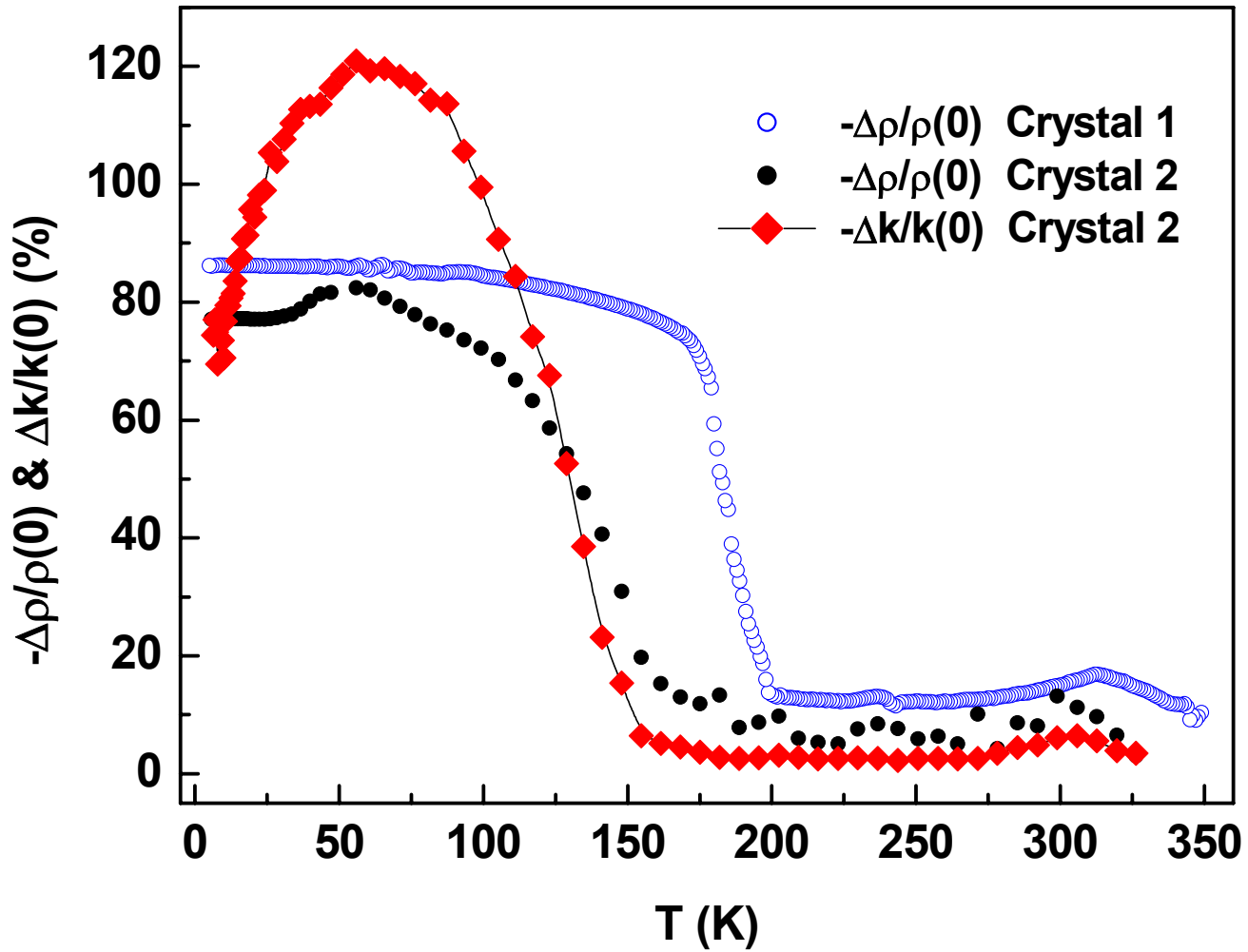
The sum of $\Delta\kappa_{\text{el}}$ and zero-field κ gives total κ



M(H) and MTC(H) in different fields

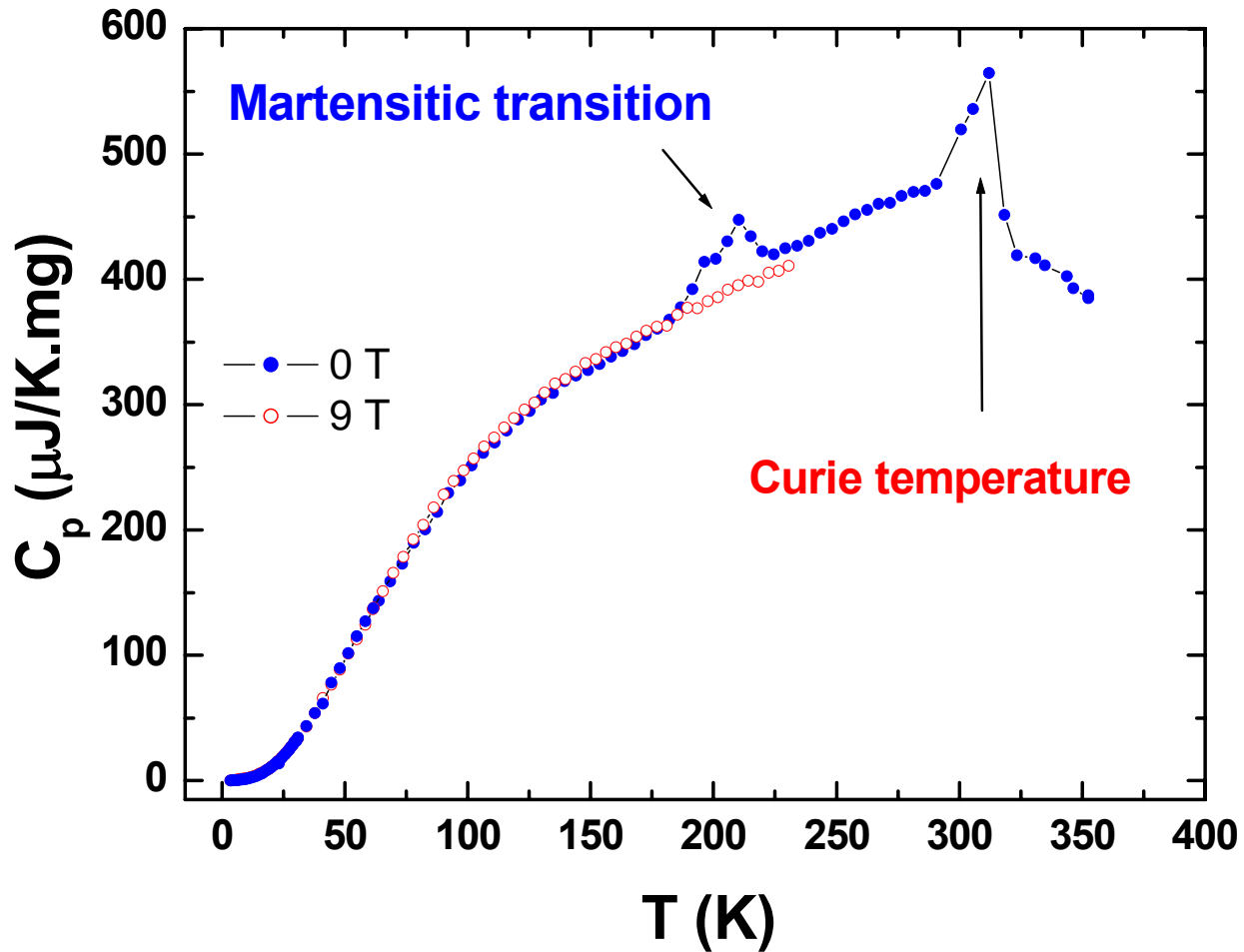


The largest magneto-thermal conductivity

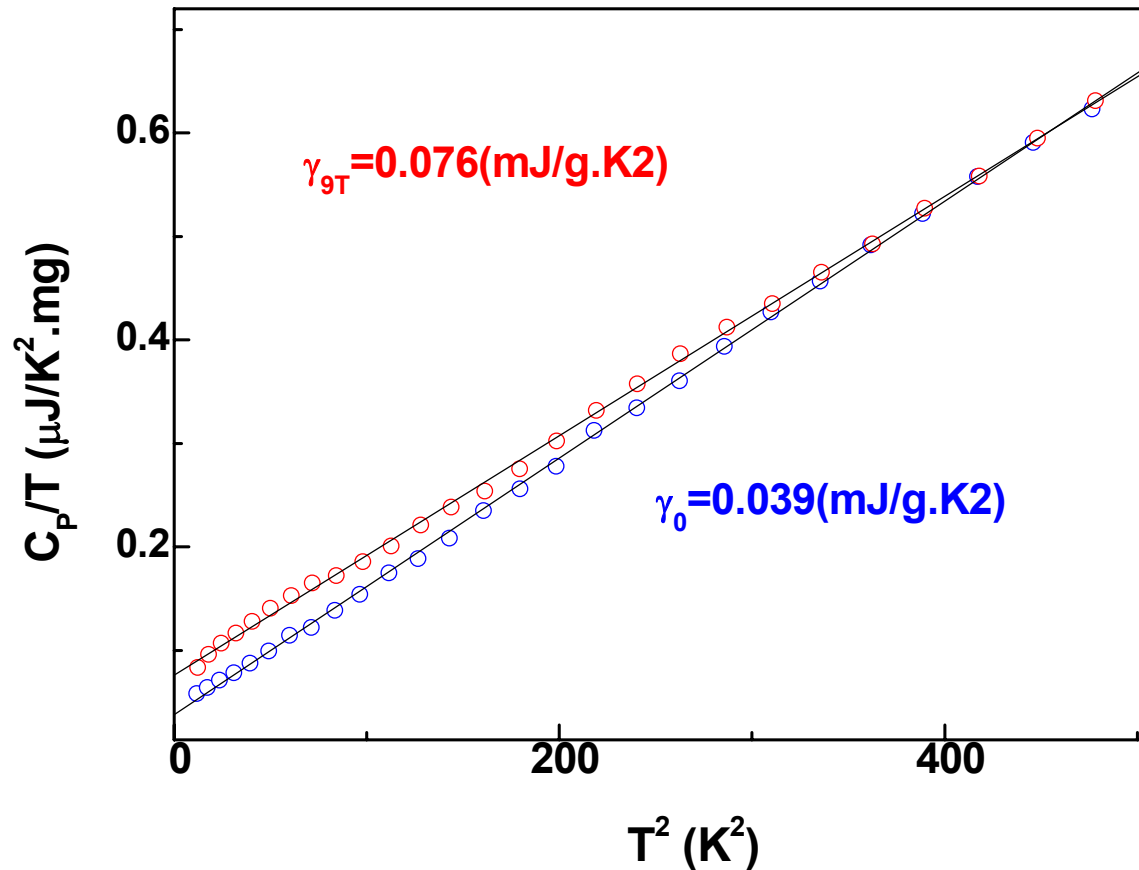


At 5K, for Crystal 1 MR =86%

Specific heat measurement



Specific heat measurement



$$C_p = \gamma T + AT^3$$

$$\gamma = V_m \left(\frac{1}{9\pi} \right)^{1/3} \left(\frac{k_B}{\hbar} \right)^2 m^* n^{1/3}$$

MR obtained from Specific Heat measurement

$$\gamma_{9T}/\gamma_0 = (n_{9T}/n_0)^{1/3} \longrightarrow n_{9T}/n_0 \approx 7.4$$

$$\rho = m / ne^2 \tau$$

$$MR = [\rho(0) - \rho(9T)] / \rho(0) = [1/n_0 - 1/n_{9T}] \cdot n_0$$

MR = 86.4%

Excellent agreement

Conclusion

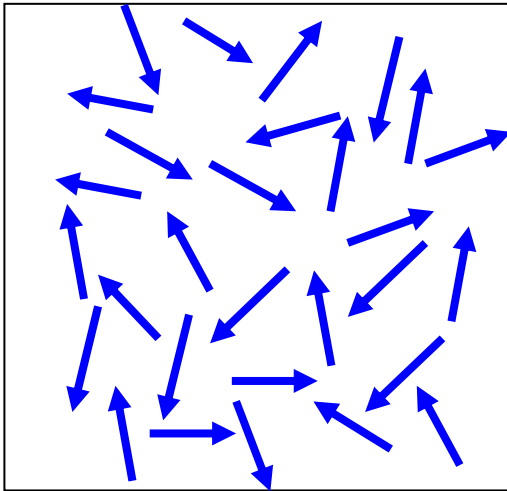
Large magnetoresistance (MR) and magnetothermal conductivity are due to the collapse of Superzone gap, when the magnetic field induced ferrimagnetic to the ferromagnetic phase transformation happens

**A combined giant inverse and
normal magnetocaloric effect for
room-temperature magnetic
cooling**

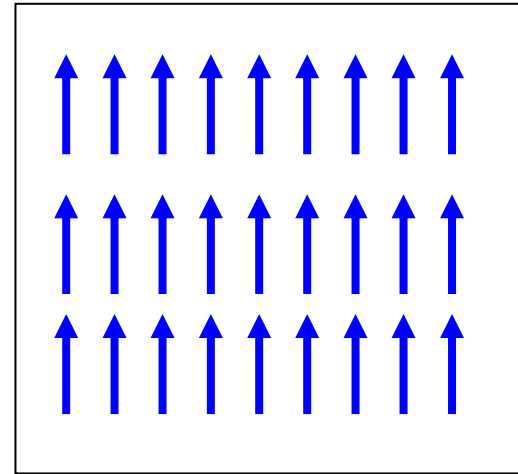
(PRB76,2007)

Magnetocaloric effect (MCE)

$H=0, T_1$
Spin disordered

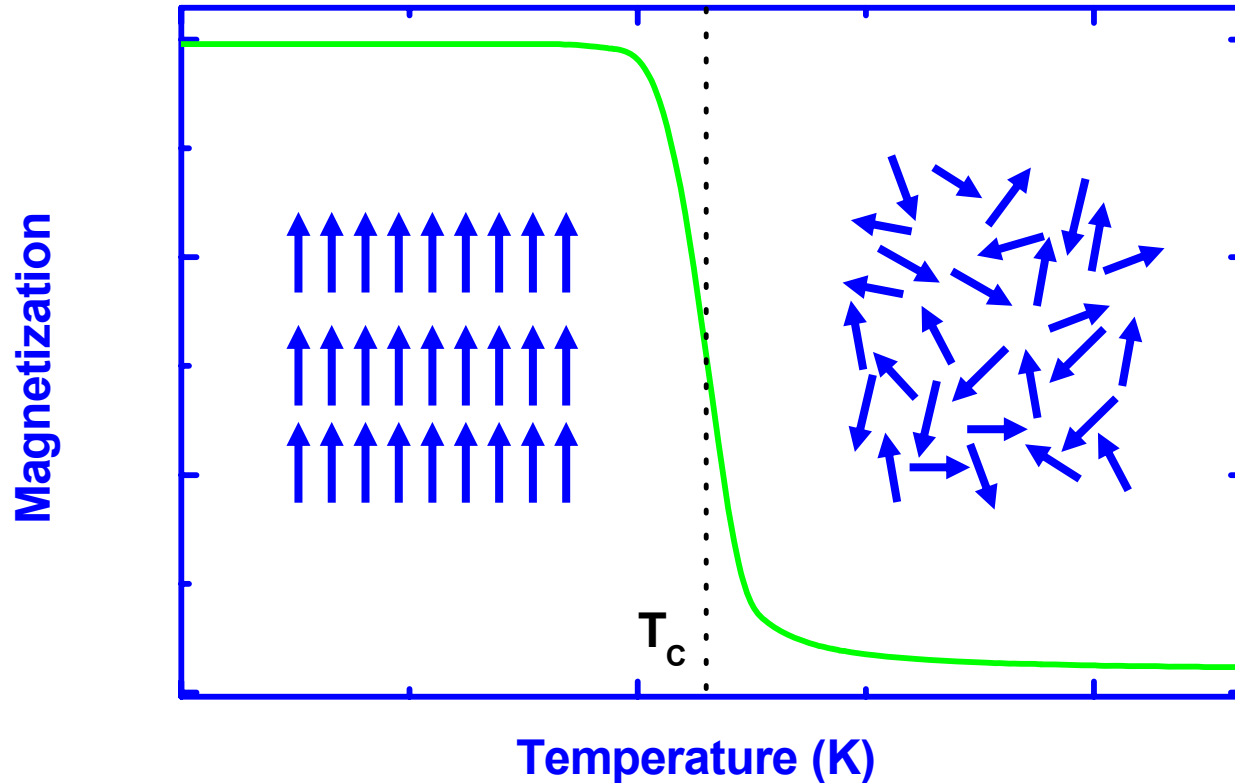


H, T_2
Spin ordered



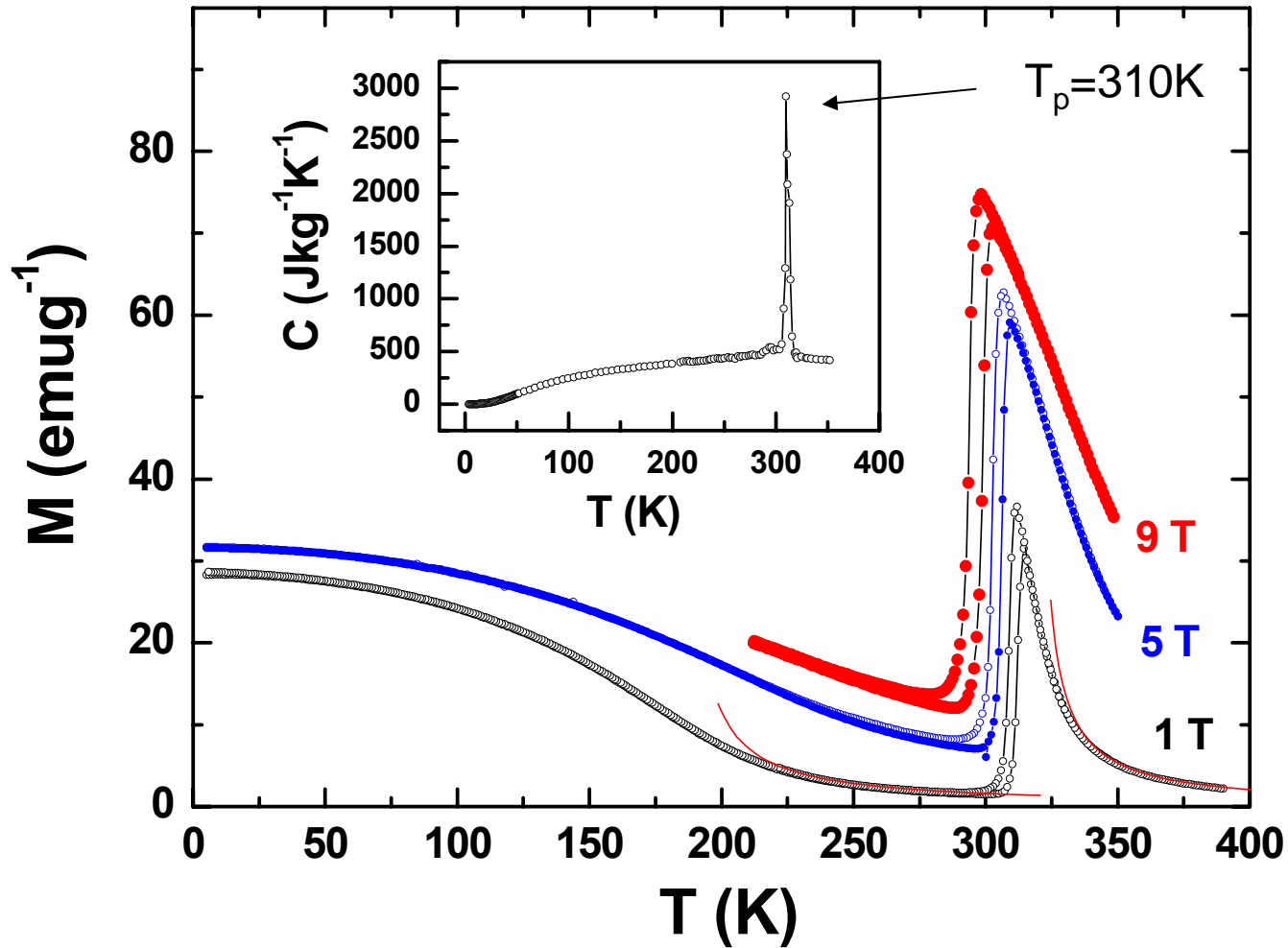
$$\Delta S_M = S_M(H_2, T) - S_M(H_1, T) = \int_{H_1}^{H_2} \left(\frac{\partial M(H, T)}{\partial T} \right)_H dH$$

Ferromagnet



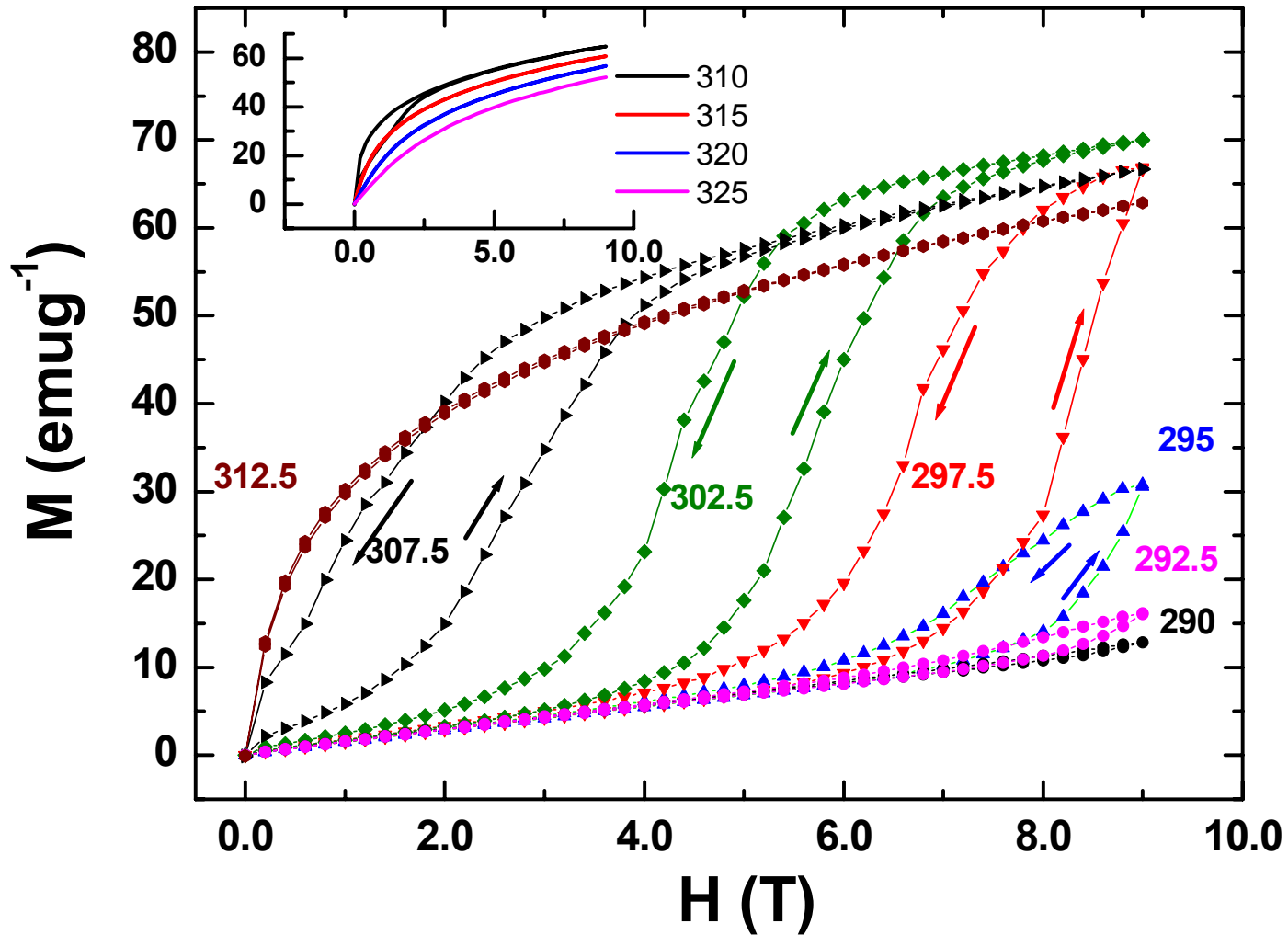
Only near the T_c , dM/dT is large, leads to a significant MCE
Room temperature application: GdGeSi, LaFeSi alloys

$\text{Ni}_{50}\text{Mn}_{33.13}\text{In}_{13.90}$ single crystal



Martensite, Ferrimagnet with $T_c = 183 \text{ K}$
Austenite, Ferromagnet with $T_c = 315 \text{ K}$

Metamagnetism vs Phase-transition



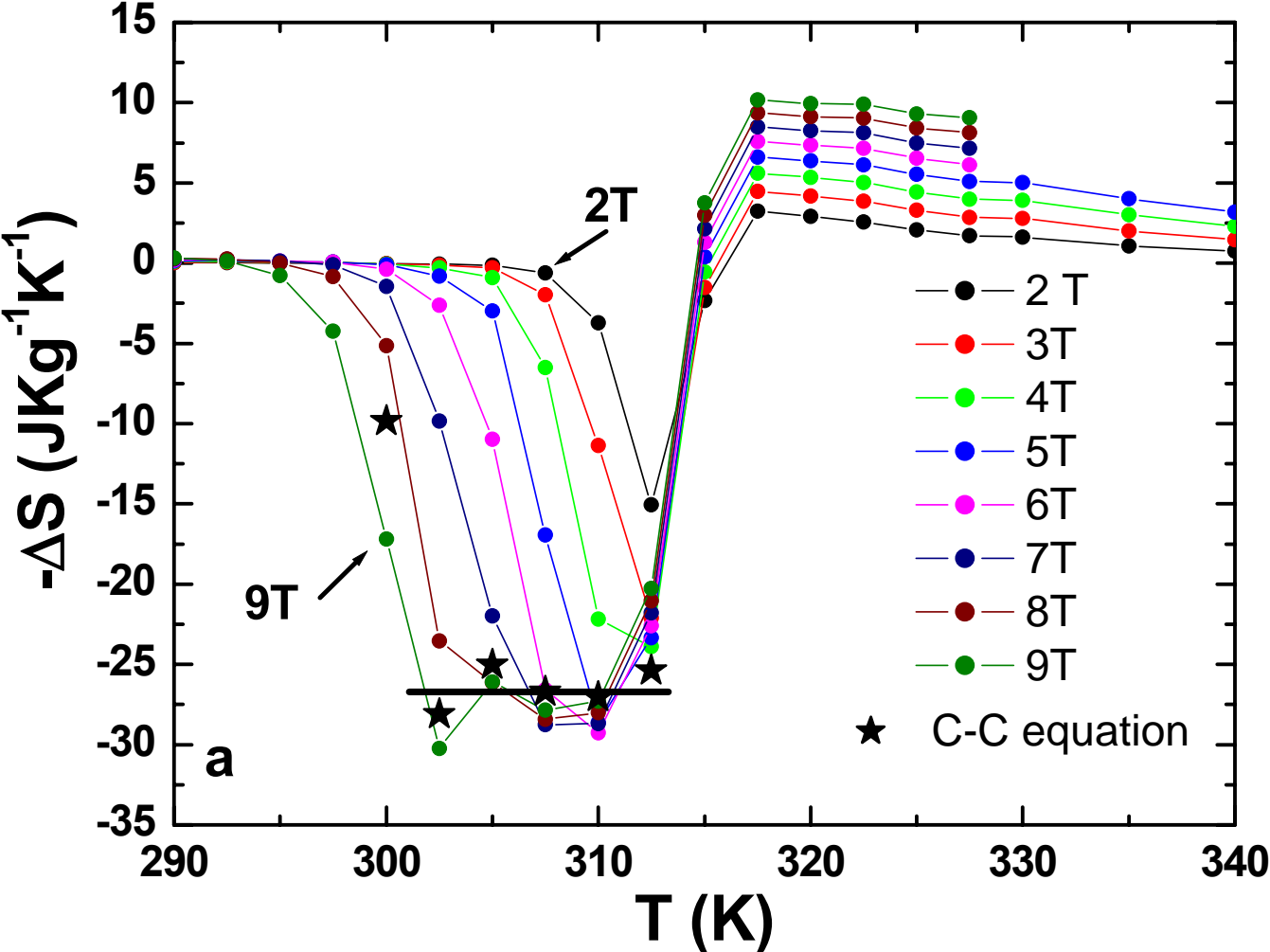
Calculation of entropy change

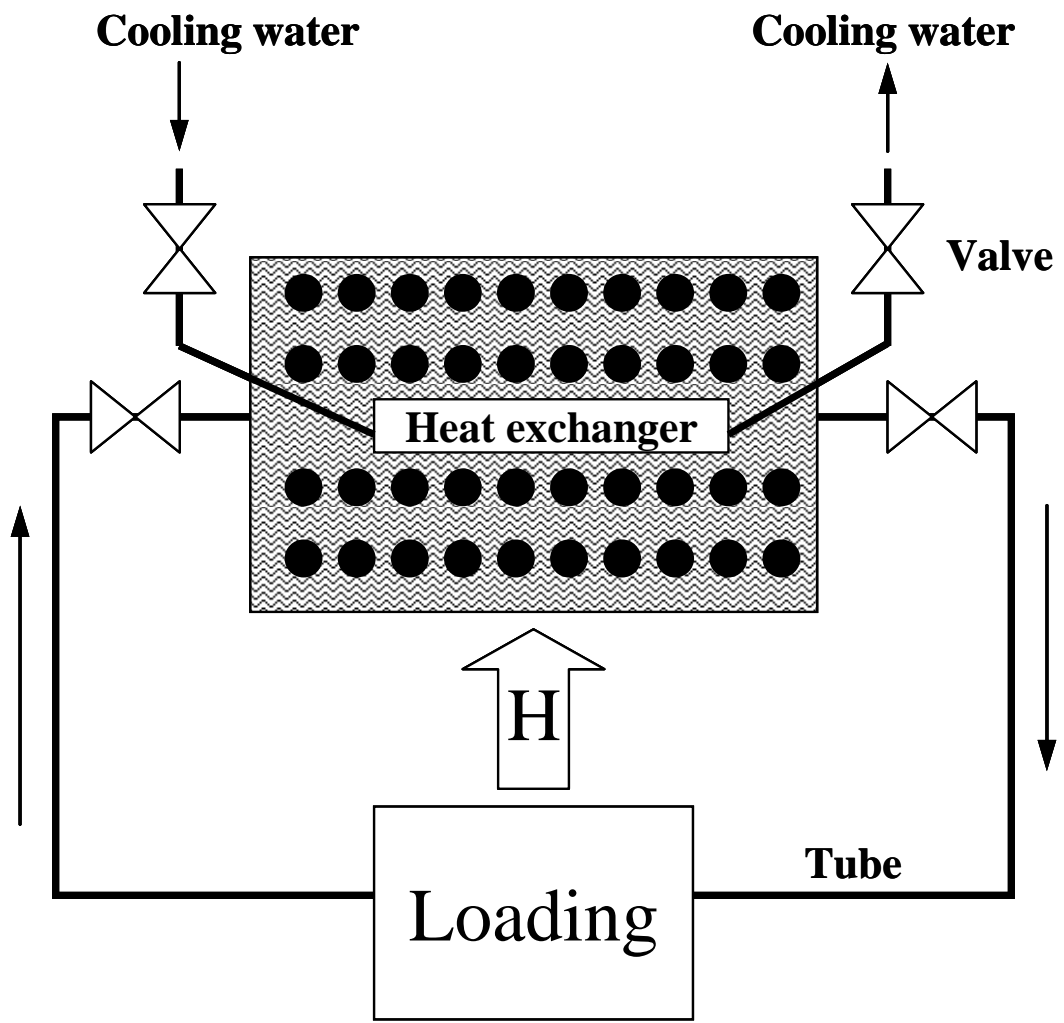
$$-\Delta S_M = \sum_i \frac{1}{T_{i+1} - T_i} (M_i - M_{i+1}) \Delta H_i$$

$$\left| \frac{\Delta \theta}{\Delta H} \right| = \left| \frac{\Delta M}{\Delta S} \right| = \textit{constant}$$

Clausius-Clapeyron equation

Entropy change vs temperature





Acknowledgement

- **Collaborators:**

- Bei Zhang, HKUST
- Guangheng Wu, Institute of Physics, Beijing
- Jinglan Chen, Institute of Physics, Beijing
- Shuyun Yu, Institute of Physics, Beijing
-

Financial supports

- 1) Hong Kong RGC
- 2) National Natural Science Foundation of China
(50571113)